dichloromaleic acid from the PCP oxidation was observed by HPLC to be degraded after 12 hours, using Li**1c** and H_2O_2 at pH 7 and 25°C. Formation of oxalate was again observed**.** In short, three successive treatments under ambient conditions of 5 mM TCP with $[Et_4N]$**1a** or Li_2**1b** and Li**1c**, along with H_2O_2, converted virtually all of the starting TCP to a mixture of small biodegradable organic acids and CO, CO_2, and HCl. Two treatments of 5 mM PCP with Li_2**1b** and Li**1c** led, within experimental error, completely to a mixture of small biodegradable organic acids and CO, CO_2, and HCl.

Complete polychlorinated dibenzodioxin and furan (210 congeners) analyses were performed on the final PCP and TCP reaction mixtures as well as the commercial starting chlorophenols. Detection limits ranged from 120 fg for 2,3,7,8-TCDD to 240 fg for 1,2,3,4,6,7,8-HpCDD. Trace quantities of dioxins and furans already present in the starting commercial PCP and TCP were not increased by the TAML-activated H_2O_2 destruction process (*5*, *8*).

The aquatic toxicities of all three Fe-TAML activators used in this study were assayed with a luminescent bacteria test (*24*). The median effective concentration (EC_{50}) values for each activator, determined with 1 mM stock solutions, were 238 mg/liter for Li_2**1b**, whereas those for $[Et_4N]$**1a** and Li**1c** were too low to be determined with 1 mM stock solutions. The LONEC values (the highest observed concentrations of activator that show no bacterial death) for $[Et_4N]$**1a**, Li_2**1b**, and Li**1c** were found to be 80, 30, and 58 mg/liter, respectively; the total catalyst concentrations used in this study were approximately 3 mg/liter. The EC_{50} and LONEC values of toxic compounds are much lower than those observed for the three Fe-TAML activators (*24*, *25*). During the course of the reaction, the Fe-TAML activators are themselves oxidatively degraded where we have suggested ideas concerning the mechanism of action of the Fe-TAML activator/H_2O_2 system (*14*, *15*). The EC_{50} for the oxidation products of Li_2**1b** was lower than that of Li_2**1b** (*26*), and the LONEC value was higher, at 140 mg/liter (30 mg/liter for activator Li_2**1b**).

Because of the importance of PCP as a recalcitrant pollutant in ground water, its oxidation was also examined in pure water at pH 7 to approximate conditions in contaminated bodies of water in the environment. In this case, a ~75% saturated solution of PCP in water (1.5 mg/25 ml at 25°C) was prepared for treatment (pH adjusted to 7.0) (*21*), but full analysis was limited by the relatively low solubility of PCP in neutral water (4 mg/50 ml at 20°C compared with the 67 mg/50 ml used above). We found that 2 μM of Li**1c** in the presence of 5 mM H_2O_2 at 25°C was required to completely degrade the PCP from the above solution in 1 hour. Analysis for chloride showed that about 94% of the PCP chlorine was liberated as mineral chloride.

The Fe-TAML/H_2O_2 system efficiently oxidizes the recalcitrant micropollutants PCP and TCP into small biodegradable organic products with substantial mineralization and does so more rapidly than the biological and chemical systems that have been previously reported. The robust nature of the Fe-TAML activators under oxidizing conditions, together with their high inherent reactivity, lead to high catalytic turnover numbers in deep oxidations of chlorophenols over the pH range of 7 to 10.5. Dioxins are not produced by the treatments. With current concerns regarding the proliferation of environmental toxins, a green process for degrading pollutants is greatly needed; this is especially true for chlorinated pollutants. The Fe-TAML/H_2O_2 system shows considerable promise for providing such a technology, subject to favorable full ecotoxicological and toxicological examinations, including persistence and bioaccumulation. Fe-TAML activators are currently undergoing industrial scale-up syntheses in preparation for commercial applications.

References and Notes

1. S. Ramamoorthy, S. Ramamoorthy, *Chlorinated Organic Compounds in the Environment* (CRC Press, Boca Raton, FL, 1997).
2. T. Hatta, O. Nakano, N. Imai, N. Takizawa, H. Kiyohara, *J. Biosci. Bioeng.* **87**, 267 (1999).
3. N. Pal, G. Lewandowski, P. M. Armenante, *Biotechnol. Bioeng.* **46**, 599 (1995).
4. K. A. McAllister, H. Lee, J. T. Trevors, *Biodegradation* **7**, 1 (1996).
5. L. G. Oeberg, C. Rappe, *Chemosphere* **25**, 49 (1992).
6. G. Mills, M. R. Hoffmann, *Environ. Sci. Technol.* **27**, 1681 (1993).
7. F. J. Benitez, J. Beltran-Heredia, J. L. Acero, F. J. Rubio, *Ind. Eng. Chem. Res.* **38**, 1341 (1999).
8. M. Fukushima, K. Tatsumi, *Environ. Sci. Technol.* **35**, 1771 (2001).
9. C. Hemmert, M. Renz, B. Meunier, *J. Mol. Catal. A Chem.* **137**, 205 (1999).
10. A. Sorokin, J.-L. Séris, B. Meunier, *Science* **268**, 1163 (1995).
11. A. Sorokin, B. Meunier, *Chem. Eur. J.* **2**, 1308 (1996).
12. A. Sorokin, S. De Suzzoni-Dezard, D. Poullain, J.-P. Noël, B. Meunier, *J. Am. Chem. Soc.* **118**, 7410 (1996).
13. A. Pifer *et al.*, *J. Am. Chem. Soc.* **121**, 7485 (1999).
14. C. P. Horwitz *et al.*, *J. Am. Chem. Soc.* **120**, 4867 (1998).
15. M. J. Bartos *et al.*, *Coord. Chem. Rev.* **174**, 361 (1998).
16. L. D. Vuocolo, thesis, Carnegie Mellon University, Pittsburgh, PA (2000).
17. T. J. Collins, *Acc. Chem. Res.* **27**, 279 (1994).
18. J. A. Hall *et al.*, in *Proceedings of the 53rd APPITA Annual Conference*, 19 to 22 April 1999, Rotorua, New Zealand (Appita, Victoria, Australia, 1999), vol. 2, pp. 455–461.
19. A. D. Ryabov, D. Mitchell, A. Ghosh, T. J. Collins, in preparation.
20. A. Hadasch, A. Sorokin, A. Rabion, B. Meunier, *New J. Chem.* **22**, 45 (1998).
21. Details of reaction conditions and product analysis are available on *Science* Online at www.sciencemag.org/cgi/content/full/296/5566/326/DC1.
22. T. Nash, *Biochem. J.* **55**, 416 (1953).
23. L. I. Simandi, M. Jaky, N. T. Son, J. Hegedus-Vajda, *J. Chem. Soc. Perkin II*, 1794 (1977).
24. J. M. Ribo, K. L. E. Kaiser, *Toxicity Assess. Int. Q.* **2**, 305 (1987).
25. K. L. E. Kaiser, J. M. Ribo, *Toxicity Assess. Int. Q.* **3**, 195 (1988).
26. The degradation reaction of the activator was initiated by adding 1 M H_2O_2 to a 1 mM solution of activator at 50°C. After 12 hours, the solution was centrifuged, and the supernatant was used for toxicity tests.

27. We thank NIH (grant GM44867-05) and the Institute for Green Oxidation Chemistry of Carnegie Mellon University for financial support, the German Deutscher Akademischer Austausch Dienst for travel support for S.S.G., the International Water Conference for a research prize to S.S.G., the Arnold and Mable Beckman Foundation for a fellowship to C.A.N., and C. Doonan for the use of analytical instruments.

21 December 2001; accepted 4 March 2002

Organic Molecules Acting as Templates on Metal Surfaces

F. Rosei,[1] M. Schunack,[1] P. Jiang,[2] A. Gourdon,[2] E. Lægsgaard,[1] I. Stensgaard,[1] C. Joachim,[2] F. Besenbacher[2]*

The electronic connection of single molecules to nanoelectrodes on a surface is a basic, unsolved problem in the emerging field of molecular nanoelectronics. By means of variable temperature scanning tunneling microscopy, we show that an organic molecule ($C_{90}H_{98}$), known as the Lander, can cause the rearrangement of atoms on a Cu(110) surface. These molecules act as templates accommodating metal atoms at the step edges of the copper substrate, forming metallic nanostructures (0.75 nanometers wide and 1.85 nanometers long) that are adapted to the dimensions of the molecule.

The adsorption of large functional molecules on surfaces plays a vital role for the emerging field of nanotechnology (*1*), in particular in areas such as molecular electronics (*2*), nanodevices (*3*), and molecular recognition (*4*). Molecular ordering is, in general, controlled by a detailed balance between intermolecular noncovalent binding forces and molecule-substrate interactions (*5, 6*). It has been inferred that complex molecules such as hexa-*tert*-butyl decacyclene (*7, 8*), C_{60} (*9, 10*), and phthalocyanine (*11*) can induce restructuring of metal surfaces accompanied by long-range mass transport. The restructuring is often

driven by cooperative molecule-substrate interactions involving many molecules, and is not directly related to the shape of individual molecules.

In this context, the scanning tunneling microscope (STM) has become a powerful tool for resolving the atomic-scale realm of surfaces. The STM tip can also be employed to manipulate single atoms and molecules in a bottom-up fashion, collectively (*12*) or one at a time (*13–16*). In this way, molecule-induced surface restructuring was revealed directly (*7, 8*) and nanostructures were engineered with atomic precision to study fundamentally interesting surface quantum phenomena (*14, 16*). Assembling functional molecular nanoelectronic devices with this serial manipulation approach is, however, extremely slow and thus technologically unattractive.

Self-assembly of molecules on surfaces, on the other hand, is a parallel and therefore technologically more promising process (*17*). For this reason, the interaction between complex organic molecules and crystal surfaces has recently been the subject of many studies, with the aim of developing applications in nanoelectronics and nanomechanical devices (*18–23*). Presently, however, it is still not possible to control self-assembly processes with atomic-scale precision. Ideally, to create functional mono-molecular or hybrid-molecular devices, it is necessary to develop an architecture for the interconnection of individual molecules, molecular devices, and wires in a planar conformation and with atomic precision to one end of nanoscale metallic contacts (*2*). In spite of the latest developments in the field of nanolithography (*24*), it has not yet been possible to create appropriate nanocontacts in an ultraclean environment more structured than a step edge (*25, 26*).

We studied the adsorption of a $C_{90}H_{98}$ molecule, known as the Lander (*25*), on a clean Cu(110) surface (*27*). At room temperature (RT), Cu kink atoms are highly mobile, as evidenced from the frizzy appearance of step edges in STM images (*28*). At low temperatures (LT), on the other hand, this mobility is frozen out, resulting in static step edges.

The Lander molecule consists of a conducting board (π-system) and four spacer legs that elevate the board from the substrate, with the aim of electronically isolating it from the surface (Fig. 1A). The conformation and anchoring of the molecules on the Cu(110) surface are studied on the atomic scale by variable temperature STM (*27, 29*). By manipulating individual molecules at LT, surprisingly, we find that a single Lander molecule can act as a template, self-fabricating metallic nanostructures at step edges. This restructuring process can be described in terms of the structure of the molecule, which reshapes a portion of the step edge, leading to the formation of a nanostructure two Cu atoms wide and eight Cu atoms long.

In Fig. 1, D and E, we present a LT (100 K), high-resolution STM image of a single Lander molecule deposited on the Cu(110) surface and a corresponding height profile (Fig. 1B) across the molecule. The STM images a Lander as four lobes arranged in either a rhomboidal or rectangular geometry. From the structure of the molecule and elastic scattering quantum chemistry (ESQC) calculations (*30*), we infer that the four lobes in the images correspond to tunneling through the spacer legs of the molecule. The two different molecular shapes found in the STM images in turn correspond to the two possible geometrical conformations of the molecule on the surface, one with the four legs arranged parallel and the other with its legs antiparallel to each other (Fig. 1).

Upon submonolayer deposition of the Lander at RT, the molecules adsorb on the surface and diffuse toward step edges, as shown in Fig. 2A. To investigate in detail the anchoring of the molecules on the surface, STM manipulation experiments were performed at temperatures ranging from 100 to 200 K on isolated molecules adsorbed on step edges, that had been deposited at RT. We used the STM tip as a tool to push the molecules away from the step edge in a gentle manner. The manipulation is obtained by reducing the resistance in the STM tunneling junction by about two orders of magnitude, from 5 gigaohms to about 0.05 gigaohms (by either increasing the tunneling current or reducing the tunneling voltage, or both), corresponding to a tip/surface approach of about 0.2 nm. By controlling the precise tip position, we are able to manipulate individual molecules one at a time along a predefined path, leaving the rest of the scan area unperturbed.

Surprisingly, such manipulation of individual molecules reveals an underlying restructuring of the monoatomic Cu steps induced by the docked molecules. A manipulation sequence is shown in Fig. 2, A through D, in which two neighboring molecules are removed from the step edge [neighbors in (A) and (C)]. A "tooth-like" metal nanostructure appears at the site where the molecules were previously attached [attachment sites in (B) and (D)]; a zoom-in with atomic resolution is shown in Fig. 2E. We can rule out that the tooth-like structures are induced by the STM tip, because no such structures are formed when we perform exactly the same manipulation at a step region where no molecules were present initially (*31*). A statistical analysis of the tooth-like nanostructure's width and length (performed on about 100 structures) yields 0.75 ± 0.05 nm (this corresponds approximately to the distance between opposite legs within a Lander) and 1.85 ± 0.35 nm (whereas the Lander is 1.7 nm long), respectively. This corresponds to a width of two atomic Cu rows aligned along the close-packed [1$\bar{1}$0]

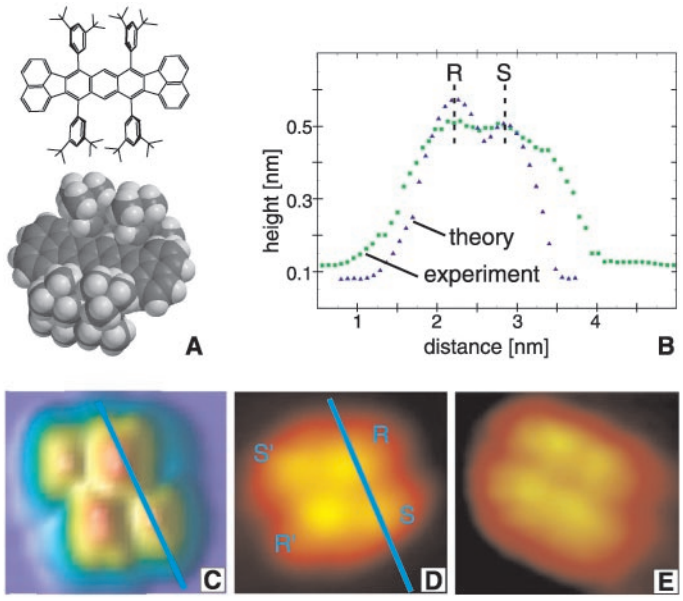

Fig. 1. (**A**) Molecular structure and ball model of the Lander molecule. The Lander is 1.4 nm long and 1.2 nm wide. It consists of a central polyaromatic board (molecular "wire"), which is terminated by a fluoranthene group, and has four 3,5-di-tert-butylphenyl "spacer legs" that elevate the central board of the molecule by a nominal distance of 0.5 nm above the substrate. The molecules are deposited on the surface by means of organic molecular beam epitaxy from a glass crucible under ultra–high vacuum conditions. (**B**) Linescan height profile taken across the lobes on the image reported in (D), and the corresponding calculated image in (C). (**C**) Calculated constant current STM image of the Lander molecule on Cu(110). (**D**) High-resolution STM image of a single Lander molecule in rhomboidal conformation on Cu(110) at LT (100 K). Image dimensions are 2 nm by 2 nm. (**E**) STM image of a single Lander molecule in rectangular conformation on Cu(110) at LT (100 K).

[1]Institute of Physics and Astronomy and CAMP, University of Aarhus, 8000 Aarhus C, Denmark. [2]CEMES – CNRS, 29 rue J. Marvig, Post Office Box 4347, F-31055 Toulouse Cedex, France.

*To whom correspondence should be addressed. E-mail: fbe@ifa.au.dk

direction, with a length of seven Cu atoms along the same direction.

Height profiles measured across the Lander molecules just before and after the manipulation sequences show that the molecules undergo a conformational change during the manipulation. Remarkably, the distances between the four lobes across the nanotooth decrease from 0.85 ± 0.25 nm in the initial configuration, in which the molecule is attached to the step edge, to 0.60 ± 0.25 in the final one, in which the molecules are moved to a flat Cu(110) terrace. In the same way, the apparent height of the molecules in the STM images decreases from 0.58 ± 0.02 to 0.45 ± 0.02 nm.

To obtain further insight into the conformational changes of the molecules, we first address how the different conformations of the molecules on the flat terrace are imaged by the STM. For the calculations, the ESQC routine was used together with a standard MM2 routine (*30, 32*) to optimize the structural rigidity and conformations of the Lander molecules on the Cu(110) terraces and on the step edges. The calculations include electronic coupling with the substrate as well as the leakage current through the four spacer legs.

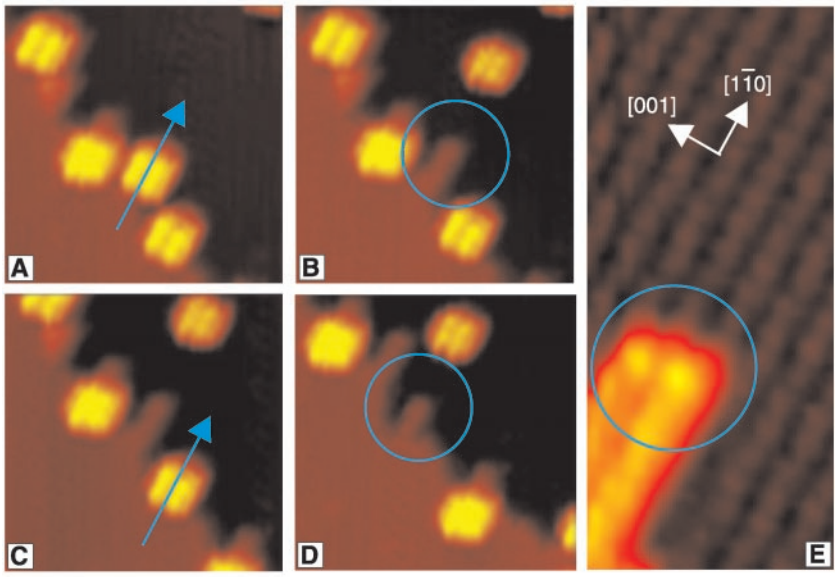

Fig. 2. (**A** to **D**) Manipulation sequence of the Lander molecules from a step edge on Cu(110). The arrows show which molecule is being pushed aside; the circles mark the tooth-like structures that are visible on the step where the molecule was docked. All image dimensions are 13 nm by 13 nm. Tunneling parameters for imaging are: $I_t = -0.47$ nA; $V_t = -1.77$ V; tunneling parameters for manipulation are: $I_t = -1.05$ nA; $V_t = -55$ mV. (**E**) Zoom-in smooth-filtered STM image showing the characteristic two-row width of the tooth-like structure (right corner) after removal of a single Lander molecule from the step edge. The Cu rows are also visible. The arrows show the directions on the surface. $I_t = -0.75$ nA; $V_t = -1.77$ V. Image dimensions are 5.5 nm by 2.5 nm.

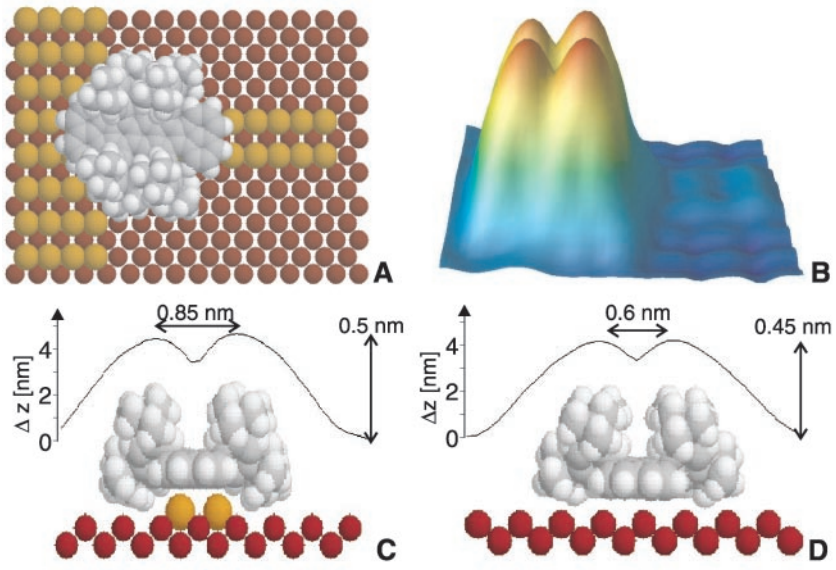

Fig. 3. Details of the conformation of the Lander molecule on the tooth. (**A**) Molecular structure, extracted from a comparison between experimental and calculated STM scans, shows that the board is parallel to the tooth. (**B**) Calculated constant-current 3D STM image. (**C**) Cross section of the tooth. (**D**) Cross section on a terrace. Tunneling parameters are: $I_t = -0.47$ nA; $V_t = -1.77$ V.

In Fig. 1, we present a calculated STM image of an isolated molecule on the flat Cu(110) terrace (Fig. 1C) as well as a line scan across the molecule (Fig. 1B), using tunneling parameters identical to the experimental ones. The agreement between theory and experiment is very good, allowing for the fact that the tip used in the simulations was atomically sharp, thereby avoiding tip convolution effects. The contrast in the STM images is mainly associated with the tunnel channels through the four spacer legs, and the molecular orbitals of the wire do not contribute to this contrast (*33*). The molecular central board is strongly attracted to the surface because of the large π-system facing the metal surface (*34*). This introduces a severe constraint on the legs, which leads to an out-of-plane distortion of each leg-board sigma bond. In turn, this has the effect of lowering the height of the legs relative to the surface.

We now focus on the molecules anchored to the tooth-like nanostructure at the step edge. From the theoretical calculations, the conformation with the Lander wire parallel to the Cu rows on the tooth is found to be more stable by 19 kcal/mol, as opposed to the conformation with the board oriented perpendicular to the nanostructure. We present in Fig. 3A the lowest energy conformation of the molecule adsorbed at the step edge on a tooth-like nanostructure consisting of two Cu rows along the [1$\bar{1}$0] direction, together with the calculated STM image (Fig. 3B). Comparing the calculated scans across the Lander on a flat terrace (Fig. 3D) and on the tooth (Fig. 3C) with experimental results, we conclude that the molecule restores a more vertical conformation of the legs when adsorbed on the tooth compared to its conformation on the flat terrace. The leg-board sigma bond almost restores its planarity relative to the board, because when the Lander is on the tooth, its central board is lifted up by more than 0.1 nm relative to the surface. This reduces the steric constraint existing on the leg-board sigma bond, leading to an increased width (0.83 versus 0.63 nm) and height (0.50 versus 0.45 nm) of the Lander in the STM image, in good agreement with the experimental findings (*34*).

The overall process for anchoring a Lander molecule to the Cu nanostructure can therefore be described as follows: When the

molecule diffuses toward the step edges at RT, it reshapes the fluctuating Cu step adatoms into the tooth-like nanostructures reported above. It is favorable for the Lander to anchor to the nanostructure at the step edge, because the gain in energy by adsorbing the molecule on the "tooth" relative to the flat terrace is higher than the energy required for creating the tooth (*35*). The dimension of the board and leg fits such that two atomic rows can be accommodated between the legs under the board. This leads to a favorable interaction between the π-system and the Cu atoms underneath. The dimensions and shape of the molecule form a perfect template for the double row of Cu atoms. The nanostructure can often extend further than the length of the molecule. This action takes place in the direction perpendicular to the steps (i.e., the close-packed direction), which is the favored direction for diffusion on Cu(110).

Upon adsorption of the molecules at LT (150 K), no restructuring of the Cu step edges is observed, and the molecules simply anchor to a step edge. At LT, the mobility of Cu kink atoms at the step edge is not high enough for the template to be effective. We can thus conclude that the process of step restructuring is thermally activated.

In conclusion, we have shown by STM manipulation that the Lander molecule locally restructures monoatomic steps, acting as a pinning center for step edge fluctuations on the Cu(110) surface. The Lander acts as a molecular template, reshaping portions of step edges into metallic nanostructures that are two atomic rows wide. Using appropriately designed molecules, this points to a new self-fabrication process at the nanoscale for integrated nanoelectronics.

References and Notes

1. J. K. Gimzewski, C. Joachim, *Science* **283**, 1683 (1999).
2. C. Joachim, J. K. Gimzewski, A. Aviram, *Nature* **408**, 541 (2000).
3. F. Moresco *et al.*, *Phys. Rev. Lett.* **86**, 672 (2001).
4. A. Kühnle, T. R. Linderoth, B. Hammer, F. Besenbacher, *Nature* **415**, 891 (2002).
5. M. Böhringer *et al.*, *Phys. Rev. Lett.* **83**, 324 (1999).
6. J. Weckesser, A. De Vita, J. V. Barth, C. Cai, K. Kern, *Phys. Rev. Lett.* **87**, 096101 (2001).
7. M. Schunack *et al.*, *Phys. Rev. Lett.* **86**, 456 (2001).
8. M. Schunack *et al.*, *Angew. Chem. Int. Ed.* **40**, 2623 (2001).
9. J. Weckesser *et al.*, *J. Chem. Phys.* **115**, 9001 (2001).
10. J. K. Gimzewski, S. Modesti, R. R. Schlittler, *Phys. Rev. Lett.* **72**, 1036 (1994).
11. M. Böhringer, R. Berndt, W. D. Schneider, *Phys. Rev. B* **55**, 1384 (1997).
12. Y. Okawa, M. Aono, *Nature* **409**, 683 (2001).
13. D. M. Eigler, C. P. Lutz, W. E. Rudge, *Nature* **352**, 600 (1991).
14. H. C. Manoharan, C. P. Lutz, D. M. Eigler, *Nature* **403**, 512 (2000).
15. S. W. Hla, L. Bartels, G. Meyer, K. H. Rieder, *Phys. Rev. Lett.* **85**, 2777 (2000).
16. K. F. Braun, K. H. Rieder, *Phys. Rev. Lett.* **88**, 096801 (2002).
17. S. Yokoyama, S. Yokoyama, T. Kamikado, Y. Okuno, S. Mashiko, *Nature* **413**, 619 (2001).
18. T. A. Jung, R. R. Schlittler, J. K. Gimzewski, H. Tang, C. Joachim, *Science* **271**, 181 (1996).
19. T. W. Fishlock, A. Oral, R. G. Egdell, J. B. Pethica, *Nature* **404**, 743 (2000).
20. Z. J. Donhauser *et al.*, *Science* **292**, 2303 (2001).
21. S. Datta *et al.*, *Phys. Rev. Lett.* **79**, 2530 (1997).
22. X. D. Cui *et al.*, *Science* **294**, 571 (2001).
23. A. R. Pease *et al.*, *Acc. Chem. Res.* **34**, 433 (2001).
24. T. Ito, S. Okazaki, *Nature* **406**, 1027 (2000).
25. V.J. Langlais *et al.*, *Phys. Rev. Lett.* **83**, 2809 (1999).
26. K. W. Hipps, *Science* **294**, 536 (2001).
27. F. Besenbacher, *Rep. Prog. Phys.* **59**, 1737 (1996).
28. M. Giesen-Seibert, R. Jentjens, M. Poensgen, H. Ibach, *Phys. Rev. Lett.* **71**, 3521 (1993).
29. E. Lægsgaard *et al.*, *Rev. Sci. Instr.* **72**, 3537 (2001).
30. P. Sautet, C. Joachim, *Chem. Phys. Lett.* **185**, 23 (1991).
31. To ascertain that the STM tip did not influence the conformation of the molecules during the manipulation process, we checked the internal distances of a great number of molecules (>100) lying on bare terraces. The values found are consistent with the ones obtained from manipulated molecules, and we therefore rule out the possibility that the conformational change may be induced by the STM tip.
32. Our ESQC routine is based on the calculation of the full scattering matrix of the STM tunnel junction. The description of this junction encompasses the surface, the adsorbate, the tip apex, and both the bulk material supporting the tip apex and the surface. Whatever the tip apex position is, 695 molecular orbitals are used to describe the electronic properties of the junction with the Lander positioned under the tip apex. The surface atoms and the Lander are described taking into account all valence molecular orbitals. Electronic interactions inside the junction are calculated using a semi-empirical Extended Hückel approximation with a double zeta basis set, in order to properly reproduce the tip apex wave function in space away from the tip apex end atom. The molecular mechanics routine used to optimize the Lander's geometry in the tunnel junction is a standard MM2 routine with a generalized potential for surface metal atoms.
33. A detailed analysis of the STM images reveals an asymmetry in the relative apparent height of the four lobes, i.e., the lobes R, R′ are imaged 0.03 nm higher than the lobes S, S′. From the calculations, we infer that the two smaller lobes (S, S′ in Fig. 1, B and C) are due each to a tunneling path through one leg only, whereas the two larger lobes (R, R′ in Fig. 1, B and C) are due to a more complete tunneling path which forms by a combination of tunneling channels building up through the two legs on the same side of the Lander.
34. T. Zambelli *et al.*, *Chem. Phys. Lett.* **348**, 1 (2001).
35. Effective Medium Theory calculations performed as in (*7*) yield an energy of 0.28 eV for the restructuring process at the step edge.

36. We acknowledge financial support from the Danish National Research Foundation through the Center for Atomic-scale Materials Physics (CAMP), from the VELUX foundation, and from the EU network "Manipulation of individual atoms and molecules" and the IST-FET project "Bottom Up Nanomachines." We thank R. Rosei for helpful discussions and T. Metcalfe for a critical reading of the manuscript.

19 December 2001; accepted 7 March 2002

The Effect of Algal Symbionts on the Accuracy of Sr/Ca Paleotemperatures from Coral

Anne L. Cohen,* Kathryn E. Owens, Graham D. Layne, Nobumichi Shimizu

The strontium-to-calcium ratio (Sr/Ca) of reef coral skeleton is commonly used as a paleothermometer to estimate sea surface temperatures (SSTs) at crucial times in Earth's climate history. However, these estimates are disputed, because uptake of Sr into coral skeleton is thought to be affected by algal symbionts (zooxanthellae) living in the host tissue. Here, we show that significant distortion of the Sr/Ca temperature record in coral skeleton occurs in the presence of algal symbionts. Seasonally resolved Sr/Ca in coral without symbionts reflects local SSTs with a temperature sensitivity equivalent to that of laboratory aragonite precipitated at equilibrium and the nighttime skeletal deposits of symbiotic reef corals. However, up to 65% of the Sr/Ca variability in symbiotic skeleton is related to symbiont activity and does not reflect water temperature.

Accurate estimates of past ocean temperature are key to establishing the sensitivity of the tropics to global climate change (*1–4*). One of the principal techniques used to derive past SSTs is the measurement of Sr/Ca ratios in the aragonite skeleton of massive reef corals (*5–8*). The technique is based on an inverse correlation between temperature and Sr/Ca in living corals that is applied to ancient specimens to reconstruct surface temperatures of past oceans. High measurement precision (*8*) and rapid sample throughput (*9*) afforded by recent technological advances have increased the appeal and utility of the Sr/Ca thermometer. Despite its wide application, paleotemperature estimates derived from coral Sr/Ca remain controversial (*10, 11*). At least nine different Sr/Ca paleotemperature equations have been published for the massive reef coral *Porites*. Among them, a Sr/Ca value of 9 mmol/mol yields a range of SSTs from 22.5°C through 28°C (*8, 12–19*). There are

Department of Geology and Geophysics, Woods Hole Oceanographic Institution (WHOI), Woods Hole, MA 02543, USA.

*To whom correspondence should be addressed. E-mail: acohen@whoi.edu

Organic Molecules Acting as Templates on Metal Surfaces

F. Rosei *et al.*

Science **296**, 328 (2002);
DOI: 10.1126/science.1069157